JOC The Journal of Organic Chemistry

Article

pubs.acs.org/joc

Reactivity of Cations and Zwitterions Formed in Photochemical and Acid-Catalyzed Reactions from *m*-Hydroxycycloalkyl-Substituted Phenol Derivatives

Nikola Cindro,[†] Ivana Antol,[†] Kata Mlinarić-Majerski,[†] Ivan Halasz,[‡] Peter Wan,[§] and Nikola Basarić*[,†]

[†]Department of Organic Chemistry and Biochemistry, and [‡]Department of Physical Chemistry, Ruđer Bošković Institute, Bijenička cesta 54, 10 000 Zagreb, Croatia

[§]Department of Chemistry, University of Victoria, Box 3065 STN CSC, Victoria, BC V8W 3V6, Canada

Supporting Information

ABSTRACT: Three *m*-substituted phenol derivatives, each with a labile benzylic alcohol group and bearing either protoadamantyl **4**, homoadamantyl **5**, or a cyclohexyl group **6**, were synthesized and their thermal acid-catalyzed and photochemical solvolytic reactivity studied, using preparative irradiations, fluorescence measurements, nanosecond laser flash photolysis, and quantum chemical calculations. The choice of *m*-hydroxy-substitution was driven by the potential for these phenolic systems to generate *m*-quinone methides on photolysis, which could ultimately drive the excited-state pathway, as opposed to forming simple benzylic carbocations in the corresponding thermal route. Indeed, thermal acid-catalyzed reactions gave the corresponding cations, which undergo rearrangement and elimination from **4**, only elimination from **5**, and substitution and elimination from **6**. On the other hand, upon photoexcitation of **4**–**6** to S_1 in a polar protic solvent, proton dissociation from the phenol, coupled with elimination of the benzylic OH (as hydroxide ion) gave zwitterions (formal *m*-quinone methides). The zwitterions exhibit reactivity different from the corresponding cations due to a difference in charge distribution, as shown by DFT calculations. Thus, protoadamantyl zwitterion has a less nonclassical character than the corresponding cation, so it does not undergo 1,2-shift of the carbon atom, as observed in the acid-catalyzed reaction.

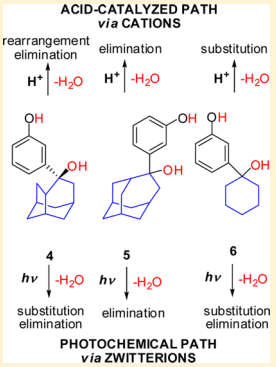

INTRODUCTION

Carbocations are reactive intermediates that have been investigated for more than 100 years.[1−3] The chemistry of carbocations blossomed in the 1960s with the discovery by Olah that simple carbenium ions can be observed at low temperatures in superacidic solutions.[4] The interest in the chemistry of carbocations was intensified with the discovery of nonclassical carbocations,[5−7] whereas significant progress was enabled later by the use of photochemical methods, particularly laser flash photolysis (LFP).[8,9] Photochemical methods for the generation of carbocations involve α- or β-cleavage of the functional groups connected to a chromophore. Formation of cations can take place via a homolytic α-cleavage of a halogen atom and subsequent electron transfer within the contact radical pair.[10] Moreover, photochemical heterolytic cleavage of a halogen−aryl bond gives a special class of aryl cations in the triplet state.[11−13] Higher reactivity of phenyl cations with olefins than with *n*-nucleophiles enabled their use in organic synthesis.[14−16]

Photochemical β-cleavage is an ubiquitous reaction in the photochemistry of ketones[17] and aromatic compounds.[18,19] Photodehydration of suitably substituted hydroxymethylphenols is a special class of β-cleavage reactions, which are coupled with excited-state proton transfer (ESPT).[20−22] Upon electronic excitation, some organic functional groups exhibit enhanced acidity or basicity,[23,24] and when the acidic and the basic sites are close, excitation can lead to excited-state intramolecular proton transfer (ESIPT).[25−28] However, if these sites are not at a short distance, proton transfer can be feasible via a relay mechanism over bridges of protic molecules.[29] Recently, we reported an example of solvent-assisted ESPT coupled with dehydration in hydroxyadamantylphenol **1** that gives rise to zwitterionic *m*-quinone methide **2**, which rearranges via 1,3-H shift and subsequent addition of water to alcohol **3** (eq 1).[30] This type of rearrangement has not

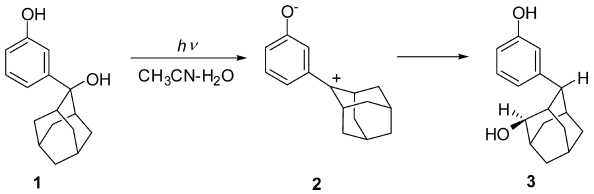

(1)

been documented in the adamantane series, whereas rearrangements of the protoadamantane skeleton in thermal solvolysis reactions via nonclassical carbocations are well-known.[31−36]

Herein, we report a more general investigation of the photochemical and thermal acid-catalyzed reactivity in a series of hydroxymethylphenols **4**–**6** bearing at the benzylic position

Received: October 3, 2015
Published: November 23, 2015

DOI: 10.1021/acs.joc.5b02297
J. Org. Chem. 2015, 80, 12420−12430

a protoadamantane, homoadamantane, or cyclohexane moiety, respectively. The molecules were designed to probe for the reaction selectivity of the photogenerated zwitterions and compare it to the reaction selectivity of carbocations formed in acid-catalyzed reactions. All investigated molecules can in principle undergo rearrangement, addition or elimination, and the selectivity should be influenced by the polycyclic skeleton. The thermal reactivity of phenols **4**–**6** was investigated by acid-catalyzed solvolysis and isolation of products, whereas photochemical reactivity was probed by preparative irradiations in the nucleophilic solvent CH_3OH, and spectroscopic investigations involving fluorescence and laser flash photolysis (LFP). The results were corroborated by DFT calculations. Both experimental and theoretical investigations on these simple systems have demonstrated that cations and zwitterions show different reactivity.

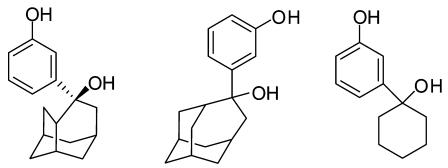

4 **5** **6**

RESULTS

Synthesis. Molecules **4** and **5** were prepared from the corresponding ketones protoadamantan-4-one[37] and homoadamantan-4-one,[38] respectively. In the first step, the ketone reacted with the Grignard reagent formed from 3-bromoanisole (Schemes 1 and 2). The methoxy groups were cleaved off subsequently by treatment with sodium thiolate, according to the modification of the known procedure.[39] In case of the proto derivative, the Grignard reaction furnished a mixture of *endo*-**7** and *exo*-methoxy product **8** in a 1:4 ratio. The major product, *exo*-isomer **8**, was separated from the mixture by column chromatography and converted to phenol **4**. The *exo*-stereochemistry in **4** was confirmed by single-crystal X-ray analysis (see Supporting Information Figure S16). Cyclohexanol derivative **6** was formed in one step from 3-bromphenol by treatment with an excess of BuLi and subsequent reaction with cyclohexanone.

Scheme 1. Synthesis of Protoadamantylphenol Derivative 4

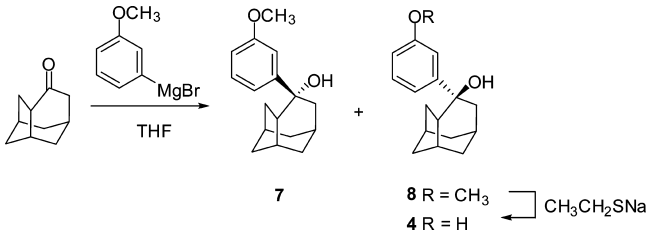

Scheme 2. Synthesis of Homoadamantylphenol Derivative 5

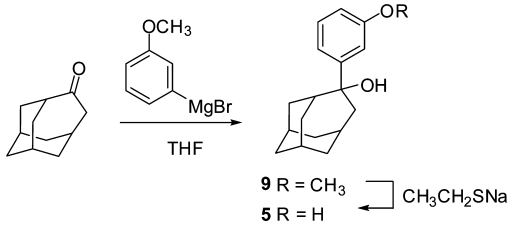

Reactivity in Acid-Catalyzed Reactions. The solvolysis of different polycyclic alcohols and the corresponding tosylates has been used in the study of rearrangement of nonclassical carbocations.[31−36] Accordingly, we performed acid-catalyzed solvolysis of **4**–**6** to investigate the reaction selectivity of the corresponding benzyl cations formed in the ground state. Acid-catalyzed solvolysis of **4** carried out in CH_3OH–H_2O (3:1) gave elimination product **10** (12%), along with the rearranged products **11** (33%) and **12** (24%), which were all isolated and characterized by NMR (eq 2). When the acid-catalyzed

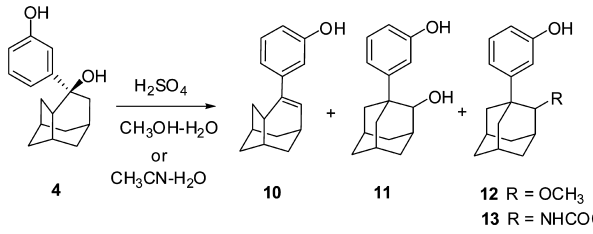

(2)

solvolysis of **4** was conducted in CH_3CN–H_2O (2:1), alkene **10** (18%), and rearranged products, alcohol **11** (22%) and acetamide **13** (30%), were isolated. Note that in the acid-catalyzed reaction, all substitution products stem from the path that involved rearrangement of the protoadamantane skeleton (Table 1).

Table 1. Products and Isolated Yields (%) after Photochemical or Thermal Acid-Catalyzed Solvolysis of Phenols 4–6

		products (%)		
reactant conditions	recovered starting material	substitution	elimination	rearrangement and substitution
4·$h\nu$[a]	**4** (10)	**16** (52), **17** (4)	**10** (12)	–[d]
4·H^+[b]		–[d]	**10** (12)	**11** (33), **12** (24)
4·H^+[c]		–[d]	**10** (18)	**11** (22), **13** (30)
5·$h\nu$[a]		–[d]	**14** (66)	–[d]
5·H^+[b]		–[d]	**14** (100)	–[d]
6·$h\nu$[a]	**6** (30)	**15** (29)	**21** (13)	–[d]
6·H^+[b]		**15** (100)	–[d]	–[d]

[a]Photolysis conducted in CH_3OH at 254 nm. [b]Solvolysis conducted in CH_3OH–H_2O (3:1) in the presence of H_2SO_4. [c]Solvolysis conducted in CH_3CN–H_2O (2:1) in the presence of H_2SO_4. [d]No product detected.

Thermal acid-catalyzed solvolysis of homoadamantyl derivative **5** gave only elimination product **14** (eq 3), isolated quantitatively and characterized by NMR. On the other hand, solvolysis of cyclohexane derivative **6** gave selectively substitution product **15** (eq 4).

Photochemical Reactivity. According to the previous reports on similar phenol derivatives,[20,21,30,40−42] irradiation of **4**–**6** in CH_3OH is anticipated to give zwitterions and the corresponding photomethanolysis products (formal substitution of OH by OCH_3). However, for derivatives **4**–**6**, more photoproducts are expected due to plausible competing elimination, rearrangement, and epimerization (in case of **4**). Therefore, we performed preparative irradiations (254 nm) of **4**–**6** in CH_3OH and isolated photoproducts. Irradiation of **4** to

DOI: 10.1021/acs.joc.5b02297
J. Org. Chem. 2015, 80, 12420−12430

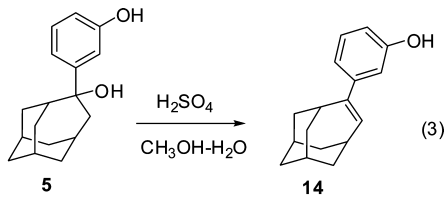

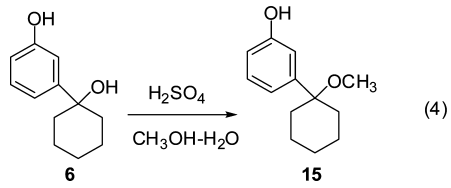

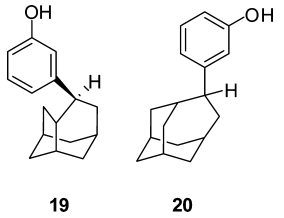

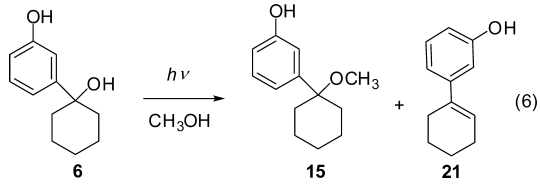

90% conversion gave four products (eq 5). The major photoproduct **16** was isolated in 52% yield. The structure of photosolvolysis product **16** was determined from NMR spectra and single-crystal X-ray analysis (see Supporting Information Figure S17). In addition to **16**, its epimer was detected (formed in 4% yield, according to NMR) but due to too small quantities could not be isolated. The elimination product **10** was isolated in the 12% yield, whereas the reduction product **18** could not be isolated. The structure of **18** was determined by catalytic hydrogenation of **10** (see the Experimental Section) wherein **18** was obtained as the major isomer in addition to some small quantities of its epimer **19**. Stereochemistry of diastereomers **18** and **19** were determined from ^{1}H NMR spectra, from the characteristic coupling constants of the H atom signal at the benzylic position and dihedral angles between the benzylic H and the vicinal H atoms, obtained by molecular modeling (see Figure S13 and Table S1). Interestingly, photomethanolysis of **4** did not give any rearranged product resulting from the 1,2-C shift in the protoadamantane skeleton, as observed in the acid-catalyzed solvolysis.

Contrary to the photochemistry of **4**, irradiation of **5** in CH_3OH to the conversion of ~30% gave only elimination product **14** (eq 3). On prolonged irradiation to higher conversion, **14** was isolated in 66% yield after the separation from high molecular weight material. Interestingly, irradiation of **5** in CH_3OH–H_2O (7:3) gave reduction product **20**, which was isolated in 18% yield. The structure of **20** was proved by independent synthesis. Homoadamantene derivative **14** was catalytically hydrogenated giving quantitatively **20**.

Irradiation of cyclohexane derivative **6** in CH_3OH until the 70% conversion was reached gave solvolysis **15** (29%) and elimination product **21** (13%, eq 6). Both products were isolated and characterized by NMR.

In summary, photosolvolysis and acid-catalyzed solvolysis of **4**–**6** gave three types of products resulting from (a) substitution, (b) elimination, or (c) rearrangement and substitution pathways. The yields of the isolated products are compiled in Table 1. Photochemical and thermal acid-catalyzed pathway result in distinctively different selectivity for derivatives **4** and **6** (but not **5**), which may be correlated with reactivity of zwitterions or cations involved in the corresponding reaction mechanisms (vide infra).

Efficiencies of photochemical transformations of **4**–**6** were determined by use of a secondary actinometer, photomethanolysis of 2-hydroxybenzyl alcohol (Φ_r = 0.23).[20] The mean values of five measurements were compiled in Table 2.

Table 2. Quantum Yields for the Photoreaction of Phenols 4–6 in CH_3OH

compound	Φ_r[a]
4	0.16 ± 0.02
5	0.025 ± 0.003
6	0.071 ± 0.007

[a]Determined by use of secondary actinometer, methanolysis of 2-hydroxybenzyl alcohol (Φ_r = 0.23)[20] in CH_3OH–H_2O 1:1. The errors correspond to averaged data of five independent measurements.

All derivatives undergo less efficient photosolvolysis than the actinometer. The finding is logical and in accord with the previous reports because the ESIPT cannot take place in the *meta*-derivatives. Involvement of a protic solvent is essential for the ESPT and dehydration.[21,40,42] Protoadamantyl derivative **4** undergoes photosolvolysis 6.4 times more efficiently than homoadamantyl **5** and 2.2 times more efficiently than cyclohexyl derivative **6**. To check for residual thermal methanolysis, solutions of **4**–**6** were kept in the dark in CH_3OH and analyzed for potential products. However, without irradiation no reaction took place.

Fluorescence Measurements. It is generally accepted that hydroxymethylphenols undergo ESPT and dehydration to the corresponding quinone methides or zwitterions from the corresponding singlet excited states.[20,21,30,40−42] To investigate the properties of phenols **4** and **5** in S_1, we conducted fluorescence measurements (Figures S1–S4). Absorption spectra of **4**–**6** taken in CH_3CN exhibit an absorption band with a maximum at ~270 nm typical for phenols corresponding to the population of S_1.[43] The emission spectra in CH_3CN have

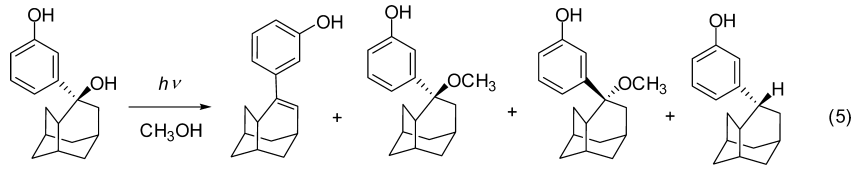

DOI: 10.1021/acs.joc.5b02297
J. Org. Chem. 2015, 80, 12420−12430

a maximum at 295 nm and exhibit no vibronic structure (Figure 1 and Figures S1–S4). Quantum yields of fluorescence for **4**

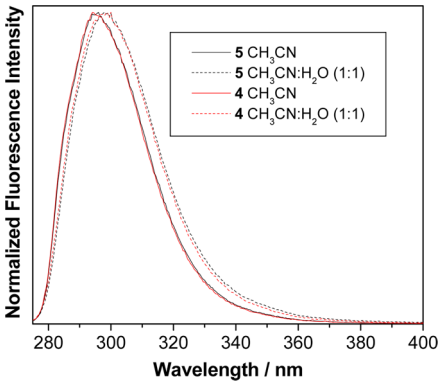

Figure 1. Normalized fluorescence spectra (λ_{ex} = 265 nm) of **4** and **5** in CH_3CN and CH_3CN–H_2O (1:4).

and **5** were measured by use of anisole in cyclohexane as a reference (see eq S1). Lifetimes were measured by time-correlated single photon counting (SPC). Similar quantum yields were measured for both **4** and **5** in CH_3CN, whereas the decay kinetics from S_1 was fitted to a monoexponential function (Table 3).

Addition of a protic solvent (H_2O) to the CH_3CN solution changes the photophysical properties of **4** and **5**. H_2O at concentrations <15 M induces weak batochromic shifts (~5 nm) and does not significantly quench fluorescence (see Figures S2 and S4). However, at higher H_2O concentrations (at ratio 1:1 or higher), fluorescence quantum yields of aqueous solutions are about one-half of those in CH_3CN (Table 3). This finding indicates that a protic solvent opens an efficient deactivation channel from S_1, ESPT to solvent molecules. Additional evidence for ESPT was obtained by SPC. The decay kinetics from S_1 in aqueous solution was fitted to a sum of two exponentials, giving decay times of phenol and phenolate formed in S_1 by ESPT to solvent (growth component with a negative pre-exponential factor).

Laser Flash Photolysis (LFP). LFP measurements were performed for polycyclic derivatives **4**, **5**, and **9** to probe for the formation of long-lived intermediates in their photochemistry (Figures S5–S12). For homoadamantyl derivative **5**, the spectra were recorded in N_2- and O_2-purged CH_3CN where ESPT cannot take place (see Figure S7). In N_2-purged solution we detected a transient absorbing at 300–600 nm with a maximum at 400 nm that decayed with $k = 2.8 \times 10^6$ s^{-1}. Because the transient was quenched with O_2 (in O_2-purged solution $k \approx 2 \times 10^7$ s^{-1}), it was assigned to the triplet state of **5**. In addition to the triplet, in both N_2- and O_2-purged solution a transient absorbing with a maximum at 400 nm was detected, decaying over longer time with $\tau > 10$ μs. According to the position of the absorption maximum, no effect of O_2 on its decay, and precedent literature,[45−47] it was assigned to the phenoxyl radical **22**.

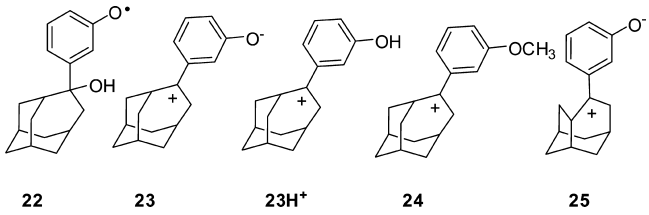

To detect cations or similar species that are expected to react fast with nucleophiles, LFP measurements were conducted in 2,2,2-trifluoroethanol (TFE). TFE is a polar but non-nucleophilic solvent in which electrophilic species live longer.[42,48,49] Contrary to CH_3CN, the transient spectra for **4**, **5**, and **9** in TFE exhibited strong absorption bands with a maximum at 360 nm that decays almost to the baseline with unimolecular kinetics with $k = (8–25) \times 10^3$ s^{-1} and is not affected by O_2 (Figure 2 and Figures S5, S8, S9, and S11). The

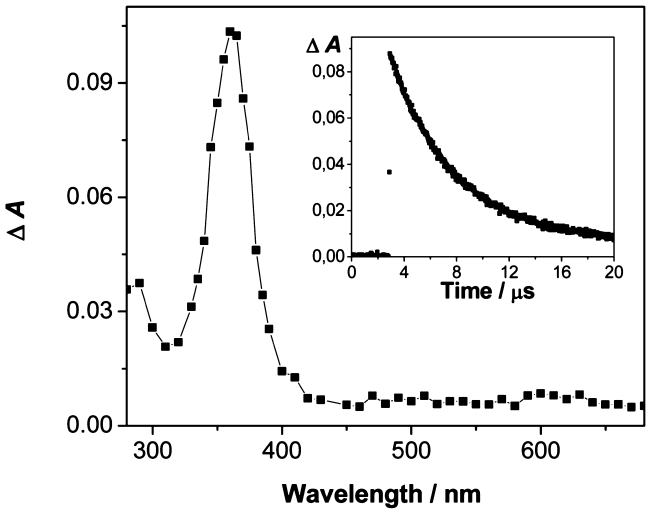

Figure 2. Transient absorption spectrum of **4** in O_2-purged TFE (delay = 400 ns). The inset shows decay at 370 nm.

transients were quenched with nucleophiles, and the rate constants were compiled in Table 4. According to the reactivity with nucleophiles, position of maxima, and precedent literature,[1,42,48,49] the observed transients detected by LFP of **4**, **5**, and **9** in TFE were assigned to zwitterions **25**, **23**, and cation **24**, respectively. The reason for assignment of the transients from **4** and **5** to zwitterions **25** and **23**, respectively, is described herein. Excitation of **5** and **9** gives rise to the

Table 3. Photophysical Properties of 4 and 5

	Φ^a (CH_3CN)	τ^b (CH_3CN)/ns	Φ^a (CH_3CN–H_2O)	τ^b (CH_3CN–H_2O)/ns
4	0.21 ± 0.01	4.84 ± 0.02	0.13 ± 0.02	3.56 ± 0.01 (97–99% phenol) 0.4 ± 0.1 (1–3% phenolate)
5	0.20 ± 0.01	4.19 ± 0.02	0.11 ± 0.01	2.80 ± 0.01 (97–98% phenol) 0.3 ± 0.1 (1–2% phenolate)

[a]Fluorescence quantum yields measured by use of anisole in cyclohexane as reference (Φ_f = 0.29).[44] Errors correspond to averaged data measured at three different wavelengths. [b]Measured by SPC. Errors correspond to those obtained by global fitting of three decays at different emission wavelengths. The contribution of phenolate is increasing at higher detection wavelength.

DOI: 10.1021/acs.joc.5b02297
J. Org. Chem. 2015, 80, 12420–12430

Table 4. Data Obtained by LFP of 4, 5, and 9 in TFE

	$\tau/\mu s$[a]	Φ_{rel}[b]	k_q (MeOH)/s^{-1} M^{-1}[c]	k_q (EtAm)/s^{-1} M^{-1}[d]
4	4.9 ± 0.3	0.52 ± 0.02	(2.0 ± 0.1) × 10^6	(1.6 ± 0.2) × 10^6
5	11.1 ± 0.3	1	(9.7 ± 0.3) × 10^5	(2.7 ± 0.3) × 10^6
9	4.2 ± 0.2	0.7 ± 0.1	(7.8 ± 0.3) × 10^6	(1.7 ± 0.1) × 10^7

[a]Lifetime of the transient in TFE. The errors correspond to averaged data of at least five decays at different wavelengths. [b]Relative efficiency for the transient formation determined from the intensities of the transient absorbance of the optically matched solutions immediately after the laser pulse. [c]Rate constant for the quenching with CH_3OH. [d]Rate constant for the quenching with ethanolamine.

Table 5. Representative Bond Lengths[a] and Charge Differences[b] in 23, 25, 26, $23H^+$, $25H^+$, and $26H^+$

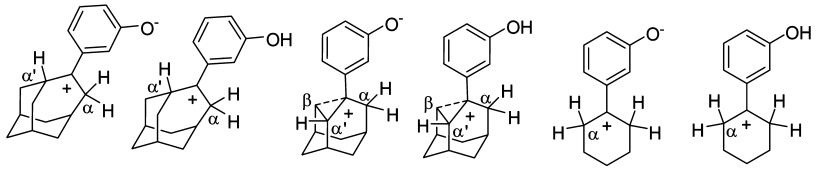

23 **23H⁺** **25** **25H⁺** **26** **26H⁺**

compound	charge difference on cationic center	charge difference on α-C and α′-C	charge difference on α-H and α′-H	distance C^+-C_α, $C^+-C_{\alpha'}$, and C^+-C_β
23	−0.18	−0.24	+0.04	1.504
		+0.29	−0.04	1.498
23H⁺	−0.18	−0.24	+0.03 or +0.06	1.490
		+0.29	+0.02	1.479
25	−0.05	−0.02	+0.01 or +0.03	1.511
		+0.15	+0.01	1.488
				2.470
25H⁺	+0.03	+0.01	+0.05 or +0.04	1.498
		+0.16	+0.01	1.462
				2.392
26	+0.60	+0.11 or −0.10	0.00 or +0.03 or	
26H⁺	+0.64	+0.02 or −0.02	0.00 or +0.06	1.482 or 1.480

[a]In angstroms. [b]The charge difference was computed between alcohols **4**–**6** and the respective intermediates.

transient species absorbing at the same wavelengths. Whereas **9** can give only cation **24**, **5** can in principle give **23** or $\mathbf{23H^+}$. However, the transient is formed more efficiently from **5**, suggesting a different mechanism of formation. It has been discussed above that free phenolic OH in S_1 undergoes ESPT to solvent giving phenolates. Moreover, the transient from **5** has 2.6 times longer lifetime, and 1 order of magnitude slower decay kinetics with nucleophiles than that from **9**. The finding is in line with better stabilization of the zwitterions through the phenoxide (O^-) at the *meta*-position that has electron-donating character (Hammet constant $\sigma_m = -0.47$), whereas OCH_3 in the *meta*-position has electron-withdrawing character (σ_m = 0.12).[44]

It is interesting to compare the lifetimes of zwitterions **23** and **25** and correlate it to the above-described photochemical reactivity of **5** and **4**. Homoadamantyl derivative **5** gives only elimination photoproduct, whereas **4** undergo competitive reactions of substitution and elimination. Thus, the decay time for **23** in TFE corresponds to the rate constant for elimination giving **14**, whereas the decay time for **25** corresponds to the sum of rate constants for the formation of **10**, **16**, and **17**.

Molecular Modeling. The major focus of the DFT calculations in the present study was to determine the structures of the assumed cationic and zwitterionic intermediates and compare their relative stabilities. The variations in charge distribution, triggered by formation of the cationic center on the benzylic carbon atom, were calculated as well. The M06-2X/6-31+G(d) method was used to optimize the structures in the gas phase. The electronic energies were recomputed by using extended 6-311++G(2df,2p) basis set. Solvation effects were added by using methanol solvent simulated within Thruhlar's SMD model. The relative stabilities of the cations were estimated by comparison of the Gibbs free energies (Δ_rG) for the reactions described in eqs 7–9:

$$\mathbf{4} + CH_3OH_2^+ \rightarrow \mathbf{25H^+} + H_2O + CH_3OH \quad \Delta_rG = 5.9\ \text{kcal mol}^{-1} \tag{7}$$

$$\mathbf{5} + CH_3OH_2^+ \rightarrow \mathbf{23H^+} + H_2O + CH_3OH \quad \Delta_rG = 5.3\ \text{kcal mol}^{-1} \tag{8}$$

$$\mathbf{6} + CH_3OH_2^+ \rightarrow \mathbf{26H^+} + H_2O + CH_3OH \quad \Delta_rG = 12.0\ \text{kcal mol}^{-1} \tag{9}$$

The corresponding zwitterions were compared using eqs 10–12:

$$\mathbf{4} \rightarrow \mathbf{25} + H_2O \quad \Delta_rG = 41.6\ \text{kcal mol}^{-1} \tag{10}$$

$$\mathbf{5} \rightarrow \mathbf{23} + H_2O \quad \Delta_rG = 40.6\ \text{kcal mol}^{-1} \tag{11}$$

$$\mathbf{6} \rightarrow \mathbf{26} + H_2O \quad \Delta_rG = 46.5\ \text{kcal mol}^{-1} \tag{12}$$

The homoadamantyl derivatives **23** and $\mathbf{23H^+}$ are the most stable in the investigated series (Δ_rG(eq 11) = 40.6 kcal mol^{-1} and Δ_rG(eq 8) = 5.3 kcal mol^{-1}, respectively). The stabilization of the positive charge at the benzylic position is achieved through resonance stabilization by phenol or phenoxide, and

DOI: 10.1021/acs.joc.5b02297
J. Org. Chem. 2015, 80, 12420–12430

Scheme 3

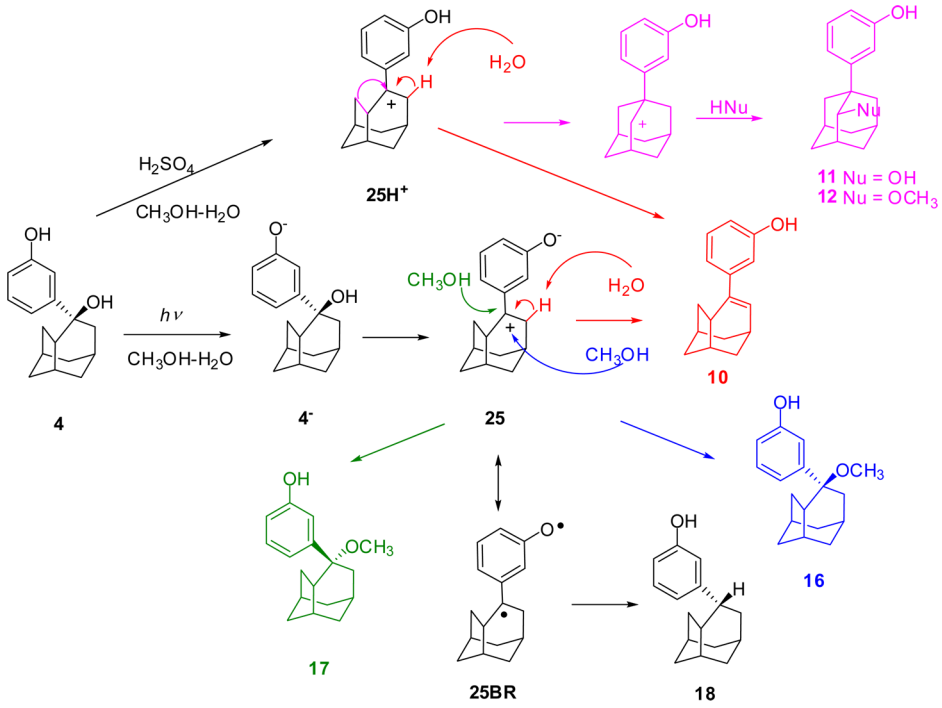

the stabilization by hyperconjugative effects with the C_α–H bonds. Thus, in **23** and **23H**$^+$, the H_α-atoms exhibit an increase of the positive charge as compared to alcohol **5**, whereas benzylic C atom exhibits an increase of the negative charge (see Table 5). Consequently, **23** and **23H**$^+$ undergo only elimination.

The $\Delta_r G$ difference between eqs 7 and 8 resembling the calculated difference in stabilization energies in **25H**$^+$ and **23H**$^+$ was only 0.6 kcal mol^{-1}. Similarly, a difference in stabilization energies calculated for the zwitterionic structures **25** and **23** amounts to only 1.0 kcal mol^{-1}. The nonclassical carbocation stabilization is present in both **25H**$^+$ and **25**, which is also evident in their stabilization with respect to **26H**$^+$ and **26** by 6.1 and 4.9 kcal mol^{-1}, respectively. The nonclassical stabilization is more pronounced in **25H**$^+$ than in **25**, which is additionally corroborated by shorter C^+–C_α and C^+–C_β bond lengths in **25H**$^+$ than in **25**. Because of the nonclassical stabilization, the C_α atom exhibits an increase of the positive charge as compared to **4**, whereas the hyperconjugative effect renders H_α-atoms more positive (see Table 5). Rearrangement to **11** and **12** was only observed in the acid-catalyzed pathway taking place via more nonclassically stabilized cation **25H**$^+$, whereas **25** gives only substitution products **16** and **17**. An increase of the positive charge at H_α-atoms leads also to the elimination product **10**, observed in both pathways.

To get more insight into the electronic structure of **25H**$^+$ and **25**, complete active space self-consistent field (CASSCF) calculations have been performed. The CASSCF energies and wave functions were calculated by using single state approach. The active space consisted of 10 active electrons and 9 orbitals mostly localized on cationic center, phenyl ring, and O atom (see Supporting Information Figures S14 and S15). The natural orbital occupation numbers are given in Figures S14 and S15 as well. It was shown that the wave function of **25H**$^+$ in the ground state has single configurational character. The weight of leading configuration ...$(60a)^2(61a)^2$ is 88.6%. Accordingly, natural occupation numbers of HOMO and LUMO orbitals are 1.90 and 0.10, respectively. In the case of zwitterionic structure **25**, the weight of the leading configuration (71.7%) is decreased with respect to its value for **25H**$^+$. Doubly excited configuration ...$(60a)^2(62a)^2$ has a weight of 15.1% leading to a redistribution of natural orbital occupation within the HOMO and the LUMO orbital. The natural orbital occupations of HOMO (1.60) and LUMO (0.41) significantly deviate from values 2 and 0, indicating a partial biradical character of structure **25**, which can explain formation of reduction product **18**. The mixing of two singlet configurations, biradical and zwitterionic, is not a surprise because similar examples can be found in literature.[50] On the contrary, for triplet biradicals it has been reported that biradical and zwitterionic wave functions do not mix.[51] It should be emphasized that the ground state of cation **25H**$^+$ and zwitterion **25** is singlet, and not the triplet state as in the cases of benzyl cations bearing strong electron-donating substituents in the meta position.[52] For these cases of meta-effect, the position of conical intersection on the reaction coordinate was shown to be responsible for the control of reactivity and selectivity.[53]

In contrast to **23**/**23H**$^+$ and **25**/**25H**$^+$ benzylic C atom in cyclohexane derivatives, **26** and **26H**$^+$ exhibit a significant increase of the positive charge as compared to alcohol **6**. The positive charge at the benzylic C atom in **26** (and **26H**$^+$) renders this position more susceptible to the attack of nucleophile as compared to protoadamantyl (**25** and **25H**$^+$) and homoadamantyl (**23** and **23H**$^+$) analogues, which results in the formation of a significant amount of substitution products, as observed in both acid-catalyzed and photochemical pathways.

DISCUSSION

Protoadamantyl phenol derivative **4** in acid-catalyzed thermal and photochemical reaction gives different type of products. Rearrangement of the protoadamantyl skeleton takes place only

DOI: 10.1021/acs.joc.5b02297
J. Org. Chem. 2015, 80, 12420–12430

in the acid-catalyzed reaction. The most probable intermediate in the acid-catalyzed reaction is cation **25H**$^+$. On the other hand, in the photochemical reaction, the probable intermediate is zwitterion **25**, in accord with the above discussion and previous reports.[21,30,40,42] The observed different reactivity of zwitterion **25** and cation **25H**$^+$ (Scheme 3) was rationalized by quantum chemical calculations. The positive charge center in zwitterion **25** is stabilized by the negative charge of the phenoxide and less delocalized as in the nonclassical carbocation **25H**$^+$. Moreover, zwitterion **25** has a noncharged resonant structure with biradical character that reduces the electrophilicity of the carbon center. Therefore, zwitterion **25** does not rearrange by 1,2-carbon shift, whereas **25H**$^+$ undergoes the rearrangement (purple pathway, Scheme 3).

Zwitterion **25** undergoes three parallel reactions, elimination to **10** (red pathway, Scheme 3), attack of nucleophiles to **16** and **17** (blue and green, Scheme 3), and radical H-abstraction pathways to **18**. The distribution between these pathways is governed by the usual factors that discriminate E1 and S_N1 reactions, including positive charge distribution on the electrophilic site, basicity versus nucleophilicity of the reagent, sterical hindrances for the attack of nucleophile to carbon or β-H atom, etc.[54] Attack of nucleophiles to **25** can take place from two sides giving substitution products **16** and **17**. The reaction is stereoselective giving **16** predominantly. The selectivity can be explained by the attack of nucleophile from the side of the six-membered ring, which positions the bulky phenyl group in the transition state to the side of the larger seven-membered ring.

Homoadamantyl phenol **5** undergoes acid-catalyzed and photochemical reaction giving the same elimination product. However, it is plausible that reactions take place via different intermediates, cation **23H**$^+$, and zwitterion **23**, respectively. LFP measurements conducted for **5** and **9** (vide supra) clearly indicate that **5** gives intermediate with different reactivity than carbocation formed from **9**. Because of the stabilization of the positive charge center in zwitterion **23** by the negative charge of the phenoxide, zwitterion **23** lives longer and reacts slower with nucleophiles than the corresponding cations **23H**$^+$ or **24**. It is interesting to note that none of the pathway gave substitution product resulting from the combination of nucleophile and electrophile. Obviously, the positive charge in **23** and **23H**$^+$ is significantly stabilized by hyperconjugative effect, rendering the β-H atom very acidic and prone to the attack of base in E1 elimination reaction.

Cyclohexyl phenol **6** gives different types of products in acid-catalyzed and photochemical pathway, contrary to homoadamantyl derivative **5**. Whereas acid-catalyzed reaction gave only substitution, photochemical pathway gave substitution and elimination products. The distribution of products could not be rationalized by quantum chemical calculations. As discussed above, the observed difference may be due to the formation of zwitterions with higher energy content than cations, resulting in less selective reactions.

CONCLUSION

Three *m*-hydroxycycloalkylphenol derivatives **4**−**6** were synthesized, and their reactivity in acid-catalyzed and photochemical solvolysis reaction was investigated experimentally and by quantum chemical calculations. Acid-catalyzed reactions give the corresponding cations which undergo rearrangement, elimination, or substitution. On the other hand, electronic excitation to S_1 in a polar protic solvent leads to phenol dissociation that is coupled by the elimination of the benzylic OH, giving zwitterions. The zwitterions exhibit different reactivity from the corresponding cations due to a different charge distribution. The most interesting finding is that the protoadamantyl zwitterion has a less nonclassical character than the corresponding cation. Consequently, protoadamantyl zwitterion gives only substitution products and does not undergo 1,2-shift of the carbon atom, as observed in the acid-catalyzed reactions. The results demonstrated herein show that photochemical and acid-catalyzed solvolysis proceed via different reactive intermediates that in some examples result in different products. The result is of particular importance in the synthetic applications of solvolysis reactions. In principle, by choosing the photochemical or acid-catalyzed solvolytic pathway, the reaction takes place via different intermediates so the selectivity can be tuned toward formation of the desired product.

EXPERIMENTAL SECTION

General. ^{1}H and ^{13}C NMR spectra were recorded at 300 or 600 MHz at rt using TMS as a reference, and chemical shifts were reported in ppm. Melting points were determined using a Mikroheiztisch apparatus and were not corrected. IR spectra were recorded on a spectrophotometer in KBr, and the characteristic peak values were given in cm^{-1}. HRMS were obtained on a MALDI TOF/TOF instrument. Irradiation experiments were performed in a reactor equipped with 13 lamps with the output at 254 nm or a reactor equipped with 8 lamps (1 lamp 8 W). During the irradiations, the irradiated solutions were continuously purged with Ar and cooled by a tap water finger-condenser. Solvents for irradiations were of HPLC purity. Chemicals were purchased from the usual commercial sources and were used as received. Solvents for chromatographic separations were used as they are delivered from supplier (p.a. grade) or purified by distillation (CH_2Cl_2).

Grignard Reaction − General Procedure. The reaction was carried out in a two-neck round-bottom flask (100 mL) under N_2 inert atmosphere equipped with a condenser and a dropping funnel. Magnesium (6 mmol), which was freshly activated prior to the reaction, was placed in the flask and suspended in THF (10 mL). In the dropping funnel was placed THF solution (15 mL) of 3-bromoanisole (5 mmol). A few drops of the solution were added to the suspension in the flask, and the reaction was initiated by adding a crystal of iodine and heating. The remaining solution in the funnel was added over 30 min at rt. After the addition was completed, the reaction mixture was refluxed until all magnesium reacted (∼1 h). The solution of the Grignard reagent was cooled to rt, and a THF solution (15 mL) of a carbonyl compound (5 mmol) was added dropvise during 1 h. After the addition was completed, the reaction mixture was refluxed for 4 h and stirred at rt overnight. The next day, to the reaction mixture was added a saturated solution of ammonium chloride (100 mL), and the layers were separated. The aqueous layer was extracted with CH_2Cl_2 (3 × 40 mL), and organic extracts were combined and dried over anhydrous $MgSO_4$. After filtration and removal of the solvent, the crude product was obtained. It was additionally purified by chromatography on silica gel using CH_2Cl_2 as eluent.

exo-4-(3-Methoxyphenyl)protoadamantan-4-ol (**8**). The Grignard reagent was prepared from 3-bromoanisol (2.00 g 10.7 mmol) and magnesium (0.28 g, 11.8 mmol), and reacted with protoadamantan-4-one (1.60 g, 10.78 mmol) to afford the crude product that was purified on a column of silica gel. After the chromatography, 1.99 g (72%) of a mixture of *endo*-**7** and *exo*-**8** isomers was obtained. The pure *exo*-isomer **8** in the form of colorless crystals was isolated from the mixture by column chromatography on silica gel using benzene−ether (98:2) as eluent (1.44 g, 52%): mp = 63−64 °C; IR (cm^{-1}, KBr) 3499, 2928, 1596, 1485, 1455, 1246, 1178, 1025, 773, 687; ^{1}H NMR ($CDCl_3$, 600 MHz) δ/ppm 7.26 (dd (t), 1H, J = 7.9 Hz), 7.09 (d, 1H, J = 7.9 Hz), 7.07 (dd (t), 1H, J = 2.2 Hz), 6.79 (dd, 1H, J = 2.2, 7.9 Hz), 3.81 (s, 3H), 2.76 (dd (t), 1H J = 9.4

DOI: 10.1021/acs.joc.5b02297
J. Org. Chem. 2015, 80, 12420−12430

Hz), 2.44 (dd, 1H, J = 6.0, 12.6 Hz), 2.40−2.35 (m, 1H), 2.28−2.23 (m, 2H), 2.19−2.12 (m, 2H), 1.83−1.79 (m, 1H), 1.74−1.68 (m, 2H), 1.58 (dd, 1H, J = 2.8, 11.0 Hz), 1.43 (dd, 1H, J = 3.7, 12.0 Hz), 1.35 (ddd (d), 1H, J = 13.1 Hz), 1.30 (dd, 1H, J = 2.4, 12.9 Hz); ^{13}C NMR ($CDCl_3$, 150 MHz) δ/ppm 159.5 (s), 150.8 (s), 129.1 (d), 118.0 (d), 112.0 (d), 111.9 (d), 76.3 (s), 55.1 (q), 45.0 (d), 42.3 (t), 42.0 (t), 39.8 (t), 36.4 (t), 35.8 (d), 33.8 (d), 32.3 (t), 28.9 (d); HRMS (MALDI-TOF) m/z $[M + K]^+$ calcd for $C_{17}H_{22}O_2K$ 297.1251; found 297.1251.

*4-(3-Methoxyphenyl)homoadamantan-4-ol (**9**).* The Grignard reagent was prepared from 3-bromoanisol (2.00 g 10.7 mmol) and magnesium (0.28 g, 11.8 mmol), and reacted with homoadamantan-4-one (1.60 g, 10.78 mmol) to afford the crude product (2.73 g) that was purified on a column of silica gel. After the chromatography, pure product **9** was isolated in the form of colorless crystals (2.00 g, 67%): mp = 130−132 °C; IR (cm^{-1}, KBr) 3494, 2887, 1594, 1445, 1241, 1024, 857, 770, 696, 547, 480; ^{1}H NMR ($CDCl_3$, 300 MHz) δ/ppm 7.25 (t, 1H, J = 8.0 Hz), 7.19−7.12 (m, 2H), 6.78 (d, 1H, J = 8.0 Hz), 3.81 (s, 3H), 2.81 (dd, 1H, J = 3.8, 15.0 Hz), 2.48 (d, 1H, J = 14.0 Hz), 2.22−2.03 (m, 3H), 2.01−1.89 (m, 4H), 1.89−1.68 (m, 4H), 1.60−1.47 (m, 4H); ^{13}C NMR ($CDCl_3$, 150 MHz) δ/ppm 159.2 (s), 152.2 (s), 128.4 (d), 119.0 (d), 112.8 (d), 111.5 (d), 81.1 (s), 55.1 (q), 50.1 (t), 44.9 (d), 38.2 (t), 37.6 (t), 36.9 (t), 31.7 (t), 31.5 (t), 31.0 (d), 27.8 (d), 27.6 (d); HRMS (MALDI-TOF) m/z $[M + K]^+$ calcd for $C_{18}H_{24}O_2K$ 311.1408; found 311.1414.

Removal of Methoxy Group − General Procedure. The reaction was carried out under N_2-atmosphere in a round-bottom flask (100 mL) equipped with a condenser and a dropping funnel, and the outlet of the N_2 from the condenser was purged through a solution of sodium ethoxide in ethanol. In the flask was placed sodium hydride (0.46 g, 20 mmol), suspended in 5 mL of dry DMF. The suspension was cooled by an ice-bath, and a solution of ethyl mercaptan (1.4 mL, 20 mmol) in DMF (5 mL) was added dropvise. When the addition was completed, the reaction mixture was stirred for 10 min and the ice-bath was removed. Methoxy derivative **8** or **9** (5 mmol) was dissolved in DMF (10 mL) and added to the reaction mixture. After the addition, the mixture was refluxed over 4 h, cooled, and poured onto H_2O (100 mL). The aqueous mixture was washed with hexane (2 × 50 mL) and acidified by a saturated solution of ammonium chloride. Extractions with EtOAc (3 × 40 mL) and CH_2Cl_2 (2 × 40 mL) were carried out, the extracts were dried over anhydrous $MgSO_4$, solid was removed by filtration, and the solvent was removed on a rotary evaporator. The reaction furnished crude product that was purified by crystallization from CCl_4−hexane.

*exo-4-(3-Hydroxyphenyl)protoadamantan-4-ol (**4**).* The reaction from **8** (1.91 g, 7.3 mmol), sodium hydride (0.70 g, 29.4 mmol), and ethyl mercaptan (2.1 mL, 29.4 mmol) furnished 2.40 g of the crude product, which was crystallized to afford the pure product in a form of colorless crystals (0.82 g, 46%): mp = 176−178 °C; IR (cm^{-1}, KBr) 3463, 3191, 2924, 1600, 1440, 1269, 1225, 1073, 984, 870, 762, 699; ^{1}H NMR (DMSO-d_6, 300 MHz) δ/ppm 9.13 (s, 1H), 7.07 (dd (t), 1H, J = 7.8 Hz), 6.91−6.86 (m, 2H), 6.57 (dd, 1H, J = 1.6, 7.6 Hz), 4.56 (s, 1H), 2.58 (dd (t), 1H, J = 8.2 Hz), 2.46−2.36 (m, 1H), 2.33−2.24 (m, 1H), 2.07 (bs, 4H), 1.74 (d, 1H, J = 13.0 Hz), 1.67−1.40 (m, 3H), 1.29 (dd (t), 2H, J = 13.0 Hz), 1.19 (d, 1H, J = 12.0 Hz); ^{13}C NMR (DMSO-d_6, 75 MHz) δ/ppm 156.9 (s), 151.9 (s), 128.5(d), 116.6 (d), 113.2 (d), 112.9 (d), 74.1 (s), 44.8 (d), 41.9 (t), 40.9 (t), 39.6 (t), 35.6 (t), 35.3 (d), 33.6 (d), 31.9 (t), 28.6 (d); HRMS (MALDI-TOF) m/z $[M - OH]^+$ calcd for $C_{16}H_{19}O$ 227.1430; found 227.1423.

*4-(3-Hydroxyphenyl)homoadamantantan-4-ol (**5**).* The reaction from **9** (0.90 g, 3.3 mmol), sodium hydride (0.32 g, 13.2 mmol), and ethyl mercaptan (0.95 mL, 13.2 mmol) furnished 1.50 g of the crude product, which was crystallized to afford the pure product in the form of colorless crystals (0.42 g, 50%): mp = 162−164 °C; IR (cm^{-1}, KBr) 3380, 3159, 2899, 1600, 1458, 1256, 1010, 867, 704; ^{1}H NMR (DMSO-d_6, 300 MHz) δ/ppm 9.14 (s, 1H), 7.07 (dd (t), 1H, J = 7.8 Hz), 7.00 (dd (t), 1H, J = 2.0 Hz), 6.96 (d, 1H, J = 7.8 Hz), 6.56 (dd, 1H, J = 2.0, 7.8 Hz), 4.81 (s, 1H), 2.61−2.50 (m, 2H), 2.13−1.95 (m, 2H), 1.91−1.65 (m, 7H), 1.59−1.33 (m, 5H); ^{13}C NMR (DMSO-d_6, 150 MHz) δ/ppm 156.5 (s), 153.3 (s), 127.9 (d), 117.4 (d), 114.0 (d), 112.5 (d), 79.3 (s), 49.3 (t), 44.7 (d), 37.5 (t), 37.3 (t), 36.7 (t), 31.4 (t), 30.9 (t), 30.6 (d), 27.4 (d), 27.3 (d); HRMS (MALDI-TOF) m/z $[M - OH]^+$ calcd for $C_{17}H_{21}O$ 241.1587; found 241.1583.

*3-(1-Hydroxycyclohexyl)phenol (**6**).* In a round-bottom three-neck flask (250 mL) equipped with a septum, a thermometer, and a N_2 inlet was dissolved 3-bromophenol (1.00 g, 5.78 mmol) in dry THF (50 mL), and the solution was cooled to −78 °C. By use of a syringe, a solution of n-BuLi in hexane (5.5 mL, c = 2.5 M, 13.75 mmol) was added slowly, taking care that the temperature did not exceed −78 °C. After the addition was completed, the solution was stirred another 10 min at −78 °C, and then a solution of dry cyclohexanone (0.60 mL, 5.78 mmol) in THF (10 mL) was added slowly. The reaction mixture was stirred and allowed to react at rt overnight. The next day a saturated solution of NH_4Cl was added and extraction with EtOAc (3 × 40 mL) was carried out. The extracts were dried over anhydrous $MgSO_4$, the solid removed by filtration, and the solvent removed on a rotary evaporator to furnish 2.0 g of the crude product. The pure product in a form of colorless crystals was obtained by column chromatography on silica gel using CH_2Cl_2 as eluent (200 mg, 18%): mp = 128−130 °C; IR (cm^{-1}, KBr) 3537, 3282, 2948, 2857, 1600, 1443, 1273, 1221, 952, 789, 697, 494; ^{1}H NMR ($CDCl_3$, 300 MHz) δ/ppm 7.21 (t, 1H, J = 7.9 Hz), 7.06 (s, 1H), 7.02 (d, 1H, J = 7.9 Hz), 6.71 (d, 1H, J = 7.9 Hz), 5.33 (s, 1H), 1.88−1.62 (m, 10H), 1.38−1.19 (m, 1H); ^{13}C NMR ($CDCl_3$, 75 MHz) δ/ppm 155.6 (s), 151.3 (s), 129.4 (d), 116.8 (d), 113.5 (d), 111.8 (d), 73.3 (s), 38.6 (t, 2C), 25.3 (t), 22.0 (t, 2C); HRMS (MALDI-TOF) m/z $[M - OH]^+$ calcd for $C_{12}H_{15}O$ 175.1117; found 175.1117.

Acid-Catalyzed Methanolysis of 4. Phenol **4** (50 mg, 2.0 mmol) was dissolved in CH_3OH (21 mL) and H_2O (7 mL). To the solution was added a few drops of conc. H_2SO_4, and the solution was stirred at rt 2 days. The reaction mixture was diluted with H_2O (100 mL), and extraction with EtOAc (3 × 40 mL) was carried out. The extracts were dried over anhydrous $MgSO_4$, the solid removed by filtration, and the solvent removed on a rotary evaporator to furnish 52 mg of the product mixture that was separated on a TLC using CH_2Cl_2 as eluent.

*4-(3-Hydroxyphenyl)protoadamant-4-ene (**10**).* Colorless crystals (13 mg, 26%); mp = 78−79 °C; IR (cm^{-1}, KBr) 3300, 3196, 2932, 2858, 1624, 1581, 1489, 1440, 1348, 1262, 1188, 777, 697; ^{1}H NMR ($CDCl_3$, 600 MHz) δ/ppm 7.18 (t, 1H, J = 8.0 Hz), 6.98 (d, 1H, J = 8.0 Hz), 6.86 (dd (t), 1H, J = 2.0 Hz), 6.69 (dd, 1H, J = 2.4, 8.0 Hz), 6.54 (dd, 1H, J = 1.4, 7.6 Hz), 4.91 (s, 1H), 3.08 (dd (t), 1H, J = 8.4 Hz), 2.55−2.48 (m, 2H), 2.35 (bs, 1H), 1.92 (dt, 1H, J = 4.6, 9.8 Hz), 1.84−1.79 (m, 1H), 1.75 (dd, 1H, J = 3.2, 11.0 Hz), 1.70 (dd, 1H, J = 3.2, 11.0 Hz), 1.66 (dt, 1H, J = 4.6, 12.0 Hz), 1.56−1.53 (m, 1H), 1.53−1.48 (m, 2H); ^{13}C NMR ($CDCl_3$, 150 MHz) δ/ppm 155.4 (s), 147.0 (s), 143.1 (s), 133.9 (d), 129.3 (d), 117.4 (d), 113.3 (d), 111.7 (d), 43.4 (t), 42.5 (t), 39.0 (d), 38.8 (d), 38.6 (t), 34.4 (d), 32.7 (d), 31.9 (t); HRMS (MALDI-TOF) m/z $[M - e]^+$ calcd for $C_{16}H_{18}O$ 226.1352; found 226.1350.

*1-(3-Hydroxyphenyl)adamantan-2-ol (**11**).* Colorless crystals (17 mg, 33%); mp = 176−178 °C; IR (cm^{-1}, KBr) 3492, 3274, 2900, 2846, 1602, 1487, 1360, 1270, 1046, 907, 774, 702; ^{1}H NMR (DMSO-d_6, 600 MHz) δ/ppm 9.01 (s, 1H), 7.04 (t, 1H, J = 7.9 Hz), 6.76 (d, 1H, J = 7.9 Hz), 6.74 (bs, 1H), 6.52 (dd, 1H, J = 1.9, 7.9 Hz), 4.12 (d, 1H, J = 4.3 Hz), 3.83 (bs, 1H), 2.30 (d, 1H, J = 11.5 Hz), 2.05 (d, 1H, J = 11.5 Hz), 1.96 (bs, 1H), 1.89−1.84 (m, 3H), 1.79 (bs, 2H), 1.67 (d, 1H, J = 12.1 Hz), 1.61 (d, 2H, J = 12.1 Hz), 1.53 (d, 1H, J = 11.3 Hz), 1.39 (d, 1H, J = 12.1 Hz); ^{13}C NMR (DMSO-d_6, 150 MHz) δ/ppm 156.8 (s), 150.1 (s), 128.3 (d), 116.2 (d), 112.9 (d), 112.0 (d), 75.0 (d), 44.0 (t), 40.4 (s), 36.5 (t), 36.0 (t), 35.2 (d), 34.3 (t), 29.9 (t), 27.9 (d), 27.7 (d); HRMS (MALDI-TOF) m/z $[M + K]^+$ calcd for $C_{16}H_{20}O_2K$ 283.1095; found 283.1089.

*1-(3-Hydroxyphenyl)-2-methoxyadamantan (**12**).* Colorless oil (12 mg, 24%); IR (cm^{-1}, KBr) 3359, 2905, 2850, 1597, 1456, 1278, 1180, 1100, 891, 768, 701; ^{1}H NMR ($CDCl_3$, 600 MHz) δ/ppm 7.16 (t, 1H, J = 7.7 Hz), 6.94 (d, 1H, J = 7.7 Hz), 6.83 (dd(t), 1H, J = 2.2 Hz), 6.62 (dd, 1H, J = 2.2, 7.7 Hz), 4.87 (s, 1H), 3.51 (bs, 1H), 3.09 (s, 3H), 2.37 (ddd, 1H, J = 2.0, 3.0, 12.4 Hz), 2.26−2.23 (m, 1H), 2.06−2.03 (m, 1H), 1.99 (ddd, 1H, J = 2.0, 3.0, 12.2 Hz), 1.97−1.90

DOI: 10.1021/acs.joc.5b02297
J. Org. Chem. 2015, 80, 12420−12430

(m, 3H), 1.79−1.72 (m, 3H), 1.69−1.63 (m, 2H), 1.49 (ddd, 1H, J = 2.0, 3.0, 12.2 Hz); ^{13}C NMR ($CDCl_3$, 150 MHz) δ/ppm 155.2 (s), 150.5 (s), 128.9 (d), 117.8 (d), 112.8 (d), 112.4 (d), 86.2 (d), 56.5 (q), 44.6 (t), 40.8 (s), 36.6 (t), 36.2 (t), 35.2 (t), 30.3 (t), 30.3 (d), 28.3 (d), 27.9 (d); HRMS (MALDI-TOF) m/z $[M + K]^+$ calcd for $C_{17}H_{22}O_2K$ 297.1251; found 297.1249.

Acid-Catalyzed Solvolysis of 4. Phenol **4** (27 mg, 1.1 mmol) was dissolved in CH_3CN (28 mL) and H_2O (12 mL). To the solution was added a few drops of conc. H_2SO_4, and the solution was stirred at rt 2 days. The reaction mixture was diluted with H_2O (100 mL), and extraction with EtOAc (3 × 40 mL) was carried out. The extracts were dried over anhydrous $MgSO_4$, the solid removed by filtration, and the solvent removed on a rotary evaporator to furnish 25 mg of the product mixture that was separated on a TLC using CH_2Cl_2 as eluent giving **10** (6 mg, 18%), **11** (6 mg, 22%), and **13** (8 mg, 30%).

*N-Acetyl-1-(3-hydroxyphenyl)-2-aminoadamantane (**13**).* Colorless crystals (8 mg, 30%); mp = 198−200 °C; IR (cm^{-1}, KBr) 3405, 3216, 2908, 2858, 1650, 1600, 1543, 1455, 1260, 782, 700, 543; ^{1}H NMR ($CDCl_3$, 300 MHz) δ/ppm 7.16 (t, 1H, J = 7.8 Hz), 6.86 (s, 1H), 6.83 (d, 1H, J = 7.8 Hz), 6.79 (bs, 1H), 6.70 (d, 1H, J = 7.8 Hz), 5.43 (d, 1H, J = 7.3 Hz), 4.43 (d, 1H, J = 7.3 Hz), 2.22 (bs, 1H), 2.13 (bs, 1H), 2.10 (d, 1H, J = 13.6 Hz), 2.01−1.93 (m, 4H), 1.88 (d, 1H, J = 12.1 Hz), 1.81−1.69 (m, 7H), 1.65 (d, 1H, J = 12.1 Hz); ^{13}C NMR ($CDCl_3$, 75 MHz) δ/ppm 169.9 (s), 156.5 (s), 148.5 (s), 129.3 (d), 116.7 (d), 113.5 (d), 112.2 (d), 56.2 (q), 46.2 (t), 39.2 (s), 36.6 (t), 36.6 (t), 35.4 (t), 32.5 (d), 30.9 (t), 28.3 (d), 27.8 (d), 23.2 (d); HRMS (MALDI-TOF) m/z $[M + Na]^+$ calcd for $C_{18}H_{23}NO_2Na$ 308.1621; found 308.1618.

Acid-Catalyzed Methanolysis of 5. Phenol **5** (30 mg, 0.11 mmol) was dissolved in CH_3OH (50 mL). To the solution was added a few drops of conc. H_2SO_4, and the solution was stirred at rt 2 days. The reaction mixture was diluted with H_2O (100 mL), and extraction with EtOAc (3 × 40 mL) was carried out. The extracts were dried over anhydrous $MgSO_4$, the solid removed by filtration, and the solvent removed on a rotary evaporator to furnish the pure product.

*4-(3-Hydroxyphenyl)homoadamant-4-ene (**14**).* Colorless crystals (28 mg, 100%); mp = 97−98 °C; IR (cm^{-1}, KBr) 3214, 2898, 2836, 1586, 1493, 1450, 1289, 1171, 893, 831, 775, 701; ^{1}H NMR ($CDCl_3$, 300 MHz) δ/ppm 7.13 (t, 1H, J = 7.9 Hz), 6.86 (d, 1H, J = 7.9 Hz), 6.76 (dd (t), 1H, J = 2.4 Hz), 6.66 (dd, 1H, J = 2.4, 7.9 Hz), 6.19 (dd, 1H, J = 1.6, 8.8 Hz), 4.83 (s, 1H), 2.80−2.76 (m, 1H), 2.48−2.38 (m, 1H), 2.20−2.10 (m, 2H), 1.91−1.86 (m, 4H), 1.84−1.78 (m, 6H); ^{13}C NMR ($CDCl_3$, 75 MHz) δ/ppm 155.2 (s), 149.7 (s), 146.5 (s), 135.3 (d), 129.1 (d), 118.0 (d), 113.0 (d), 112.4 (d), 37.1 (d), 36.5 (t), 33.9 (t, 2C), 33.8 (t, 2C), 32.0 (d), 29.3 (d, 2C); HRMS (MALDI-TOF) m/z $[M - e]^+$ calcd for $C_{17}H_{20}O$ 240.1509; found 240.1515.

Acid-Catalyzed Methanolysis of 6. Phenol **6** (60 mg, 0.31 mmol) was dissolved in CH_3OH (50 mL). To the solution was added a few drops of conc. H_2SO_4, and the solution was stirred at rt 2 days. The reaction mixture was diluted with H_2O (100 mL), and extraction with EtOAc (3 × 40 mL) was carried out. The extracts were dried over anhydrous $MgSO_4$, the solid removed by filtration, and the solvent removed on a rotary evaporator to furnish the pure product.

*1-Methoxy-1-(3-hydroxyphenyl)cyclohexane (**15**).* Colorless crystals (64 mg, 100%); mp = 96−98 °C; IR (cm^{-1}, KBr) 3304, 2933, 1617, 1453, 1282, 1221, 1167, 1057, 923, 862, 814, 783, 704; ^{1}H NMR ($CDCl_3$, 600 MHz) δ/ppm 7.21 (t, 1H, J = 7.7 Hz), 7.06 (dd (t), 1H, J = 2.4 Hz), 6.92 (d, 1H, J = 7.7 Hz), 6.77 (dd, 1H, J = 2.4, 7.7 Hz), 6.20 (s, 1H), 3.02 (s, 3H), 2.02 (d, J = 9.6 Hz), 1.75−1.67 (m, 6H), 1.61−1.55 (m, 2H), 1.30−1.21 (m, 1H); ^{13}C NMR ($CDCl_3$, 150 MHz) δ/ppm 156.2 (s), 147.3 (s), 129.4 (d), 118.0 (d), 114.2 (d), 112.8 (d), 78.3 (s), 49.4 (q), 35.2 (t, 2C), 25.4 (t), 21.8 (t, 2C); HRMS (MALDI-TOF) m/z $[M + Na]^+$ calcd for $C_{13}H_{18}O_2Na$ 229.1199; found 229.1198.

Photochemical Experiments − General. In a quartz vessel was placed a CH_3OH or CH_3OH−H_2O (3:1) solution (100 mL, $c \approx 10^{-3}$ M) of compounds **4**−**6** (∼100 mg), which was irradiated in a Rayonet reactor using 10 lamps at 254 nm for 20 min. Prior to and during the irradiation, the solution was continuously purged with a stream of Ar and cooled by a coldfinger condenser. After the irradiation, CH_3OH was removed on a rotary evaporator, and the residue was chromatographed on a TLC using CH_2Cl_2 or CH_2Cl_2−CH_3OH (2.5%) as eluent.

Irradiation of **4** (82 mg, 0.34 mmol) in CH_3OH (100 mL) for 20 min gave a crude mixture that was separated on TLC giving unreacted **4** (9 mg, 11%), **10** (10 mg, 12%), **16** (43 mg, 52%), **17** (3 mg, 4%), and **18** (4 mg, 5%).

*exo-4-Methoxy-4-(3-hydroxyphenyl)protoadamantane (**16**).* Colorless crystals (43 mg, 52%); mp = 118−120 °C; IR (cm^{-1}, KBr) 3304, 2917, 2858, 1692, 1580, 1486, 1445, 1264, 1181, 888, 776, 689; ^{1}H NMR ($CDCl_3$, 600 MHz) δ/ppm 7.20 (t, 1H, J = 8.0 Hz), 7.03 (dd (t), 1H, J = 2.0 Hz), 6.95 (d, 1H, J = 8.0 Hz), 6.77 (dd, 1H, J = 2.2, 8.0 Hz), 6.17 (s, 1H), 2.94 (s, 3H), 2.91 (dd (t), 1H, J = 8.8 Hz), 2.38 (dd, 1H, J = 5.7, 12.3 Hz), 2.34 (dd, 1H, J = 8.3, 15.0 Hz), 2.31−2.27 (m, 1H), 2.16−2.10 (m, 2H), 2.05 (dd, 1H, J = 1.3, 15.0 Hz), 1.81−1.68 (m, 3H), 1.57 (dd, 1H, J = 3.0, 11.0 Hz), 1.40 (d, 1H, J = 12.1 Hz), 1.34 (d, 2H, J = 12.8 Hz); ^{13}C NMR ($CDCl_3$, 150 MHz) δ/ppm 156.1 (s), 146.9 (s), 128.8 (d), 119.2 (d), 114.2 (d), 114.1 (d), 81.9 (s), 49.8 (q), 42.3 (t), 40.7 (d), 39.7 (t), 38.7 (t), 36.2 (t), 35.9 (d), 33.8 (d), 32.3 (t), 28.8 (d); HRMS (MALDI-TOF) m/z $[M - OCH_3]^+$ calcd for $C_{16}H_{19}O$ 227.1430; found 227.1435.

*endo-4-Methoxy-4-(3-hydroxyphenyl)protoadamantane (**17**).* Colorless crystals (3 mg, 4%); the compound was not pure enough for the characterization. The yield was calculated from the weight of the mixture and the relative ratio of the OCH_3 signal intensities in ^{1}H NMR spectrum.

*endo-4-(3-Hydroxyphenyl)protoadamantane (**18**).* Colorless crystals (4 mg, 5%); the compound was not pure enough for the characterization. For the assignation of stereochemistry, see the Supporting Information. HRMS (MALDI-TOF) m/z $[M - H]^+$ calcd for $C_{16}H_{19}O$ 227.1430; found 227.1427.

Irradiation of **5** (86 mg, 0.33 mmol) in CH_3OH (150 mL) for 20 min gave a crude mixture that was filtered through a plug of florisil to give pure **14** (57 mg, 66%).

Irradiation of **5** (100 mg, 0.39 mmol) in CH_3OH−H_2O (3:1, 150 mL) for 150 min gave a crude mixture that was separated on TLC using CH_2Cl_2 as eluent to give **20** (18 mg, 18%).

*4-(3-Hydroxyphenyl)homoadamantane (**20**).* Colorless crystals (18 mg, 18%); mp = 108−110 °C; IR (cm^{-1}, KBr) 3260, 2903, 2844, 1590, 1484, 1455, 1267, 869, 757; ^{1}H NMR ($CDCl_3$, 600 MHz) δ/ppm 7.13 (t, 1H, J = 7.6 Hz), 6.85 (d, 1H, J = 7.6 Hz), 6.77 (dd (t), 1H, J = 1.8 Hz), 6.62 (dd, 1H, J = 7.6, 1.8 Hz), 4.66 (s, 1H), 3.02 (t, 1H, J = 9.1 Hz), 2.26−2.20 (m, 1H), 2.20−2.15 (m, 1H), 2.09 (dd(t), 1H, J = 5.9 Hz), 2.00−1.89 (m, 5H), 1.86 (d, 1H, J = 14.0 Hz), 1.79 (dd, 1H, J = 10.1, 14.5 Hz), 1.73−1.67 (m, 2H), 1.64 (d, 1H, J = 14.5 Hz), 1.58−1.54 (m, 3H); ^{13}C NMR ($CDCl_3$, 150 MHz) δ/ppm 155.3 (s), 151.3 (s), 129.2 (d), 120.0 (d), 114.3 (d), 112.2 (d), 50.9(d), 42.1 (t), 41.6 (t), 41.5 (t), 38.8 (d), 36.9 (t), 34.3 (t), 31.1 (d), 31.0 (t), 27.5 (d), 27.5 (d); HRMS (MALDI-TOF) m/z $[M + Ag]^+$ calcd for $C_{17}H_{22}OAg$ 349.0716; found 349.0717.

Irradiation of **6** (106 mg, 0.34 mmol) in CH_3OH (130 mL) for 40 min gave a crude mixture that was separated on TLC giving unreacted **6** (32 mg, 30%), **15** (32 mg, 29%), and **21** (14 mg, 31%).

*1-(3-Hydroxyphenyl)cyclohex-1-ene (**21**).* Colorless oil (14 mg, 13%); IR (cm^{-1}, KBr) 3345, 2940, 1589, 1450, 1286, 1191, 774, 698; ^{1}H NMR ($CDCl_3$, 300 MHz) δ/ppm 7.16 (t, 1H, J = 8.0 Hz), 6.96 (d, 1H, J = 8.0 Hz), 6.84 (s, 1H), 6.68 (dd, 1H, J = 2.0, 8.0 Hz), 6.13−6.08 (m, 1H), 4.86 (s, 1H), 2.41−2.32 (m, 2H), 2.23−2.14 (m, 2H), 1.81−1.59 (m, 4H); ^{13}C NMR ($CDCl_3$, 150 MHz) δ/ppm 155.3 (s), 144.4 (s), 136.0 (s), 129.2 (d), 125.0 (d), 117.5 (d), 113.3 (d), 111.8 (d), 27.2 (t), 25.7 (t), 22.9 (t), 22.0 (t); HRMS (MALDI-TOF) m/z $[M + Ag]^+$ calcd for $C_{12}H_{14}OAg$ 281.0090; found 281.0081.

Hydrogenation − General Procedure. Alkene ∼40 mg was dissolved in methanol (30 mL). To the solution was added 10% Pd/C, and the mixture was hydrogenated in a Paar apparatus under H_2 pressure of 60 psi over 5 days. When the reaction was over, the catalyst was filtered off and the solvent removed on a rotary evaporator to afford a crude product that was purified by column chromatography on silica gel eluted with CH_2Cl_2.

DOI: 10.1021/acs.joc.5b02297
J. Org. Chem. 2015, 80, 12420−12430

In the hydrogenation of homoadamantane derivative **14**, almost pure **20** was obtained in quantitative yield, while hydrogenation of protoadamantane derivative **10** yielded almost quantitatively the mixture of *endo* **18** and *exo* **19** (4:1) diastereomers.

Quantum Yields for the Photomethanolysis Reaction. Quantum yield was determined by use of methanolysis of 2-hydroxybenzyl alcohol in CH_3OH-H_2O (1:1) as a secondary actinometer (Φ = 0.23).[20] Phenols **4** (10.00 mg), **5** (10.56 mg), and **6** (7.86 mg) were dissolved in CH_3OH (25 mL), whereas actinometer (5.08 mg) was dissolved in CH_3OH-H_2O (1:1, 25 mL). Concentrations of actinometer and phenols **4**–**6** were 1.64×10^{-3} M. The solutions were purged with Ar for 20 min and irradiated under the same conditions in a Rayonet reactor equipped with 9 lamps at 254 nm for 10 min. The composition after the irradiation was analyzed by HPLC.

Steady-State and Time-Resolved Fluorescence Measurements. Steady-state measurements were performed with a QM-2 fluorimeter (PTI). The samples were dissolved in cyclohexane, CH_3CN, or CH_3CN-H_2O (1:1), and the concentrations were adjusted to absorbances of less than 0.1 at the excitation wavelengths of 260, 265, or 270 nm. Solutions were purged with nitrogen for 30 min prior to analysis. Measurements were performed at 20 °C. Fluorescence quantum yields were determined by comparison of the integral of the emission bands with that of anisole in cyclohexane (Φ_F = 0.29).[44] Typically, three absorption traces were recorded (and averaged) and three fluorescence emission traces were collected by exciting the sample at 260, 265, and 270 nm. Three quantum yields were calculated (eq S1), and the mean value was reported.

Fluorescence decays, collected over 1023 time channels, were obtained on an Edinburgh Instruments OB920 single photon counter using light emitting diode for excitation at 265 nm. The instrument response functions (using LUDOX scatterer) were recorded at the same wavelengths as the excitation wavelength and had a half width of ~0.2 ns. Emission decays were recorded at 295, 330, and 350 nm. The counts in the peak channel were 3×10^3. The time increment per channel was 0.049 ns. Obtained histograms were fit as sums of exponentials using global Gaussian-weighted nonlinear least-squares fitting based on Marquardt–Levenberg minimization implemented in the Fast software package from Edinburgh Instruments. The fitting parameters (decay times and pre-exponential factors) were determined by minimizing the global reduced chi-square χ^2, and graphical methods were used to judge the quality of the fit that included plots of the weighted residuals versus channel number.

Laser Flash Photolysis (LFP). All LFP studies on a system previously described[55] employed as an excitation source a Quanta-Ray Lab 130-4 pulsed Nd:YAG laser at 266 nm from Spectra Physics (<20 mJ per pulse), with a pulse width of 10 ns. Static cells (7 mm × 7 mm) were used, and the solutions were purged with nitrogen or oxygen for 20 min prior to performing the measurements. Absorbances at 266 nm were ~0.3–0.4.

Computational Details. Calculations of **19** and **20** were performed using Gaussian 03 software.[56] Calculations of reactive intermediates and the associated reaction Gibbs energies were performed by using M06-2X[57] density functional in conjunction with Pople 6-31+G(d,p) basis set for geometry optimizations and vibrational analysis in the gas phase. The extended 6-311++G-(2df,2pd) bass set was used for computation of energies. Solvation effects have been estimated by immersing the molecules into a dielectric continuum with ε = 32.613 as defined in the Gaussian 09 program package[58] for methanol as a solvent. Trular's SMD model was used.[59] All calculations were carried out on the Isabella cluster (Isabella.srce.hr) at the University of Zagreb Computing Center (SRCE) and visualized by the VEGA-ZZ[60] and Molden[61] programs. The complete Cartesian geometries and the Mulliken partial atomic charges in all of the optimized structures are available in Table S4.

Single-Crystal X-ray Measurements and Structure Determinations. Single-crystal diffraction data were collected from the crystal glued on a glass fiber tip. Diffraction intensity data were collected by ω-scans on an Oxford Diffraction Xcalibur 3 using graphite-monochromated Cu Kα radiation (λ = 1.54 Å) and reduced using the CrysAlis program package.[62] The structures were solved by direct methods using SHELXS.[63] The refinement procedure by full-matrix least-squares methods based on F^2 values against all reflections included anisotropic displacement parameters for all non-H atoms. The positions of H atoms each riding on its parent carbon atom were determined on stereochemical grounds. Hydrogen atoms bonded to oxygen atoms were located from difference Fourier map and isotropically refined. Refinements were performed using SHELXL-97.[63] The SHELX programs operated within the WinGX suite.[64] General and crystal data are given in the cif files, which are available through the Cambridge Structural Database with deposition numbers 1427871 and 1427872. A copy of this information may be obtained free of charge from the director, CCDC, 12 Union Road, Cambridge, CB2 1EZ, UK (fax, +44 1223 336 033; e-mail, deposit@ccdc.cam.ac.uk; or http://www.ccdc.cam.ac.uk). Molecular graphics were done with ORTEP.[65]

■ ASSOCIATED CONTENT

Supporting Information

The Supporting Information is available free of charge on the ACS Publications website at DOI: 10.1021/acs.joc.5b02297.

Fluorescence spectra of **4** and **5**, LFP data, computational results, crystallographic parameters for **4** and **16**, and ^{1}H and ^{13}C NMR spectra of new compounds (PDF)

X-ray data for compound **4** (CIF)

X-ray data for compound **16** (CIF)

■ AUTHOR INFORMATION

Corresponding Author

*E-mail: nbasaric@irb.hr.

Notes

The authors declare no competing financial interest.

■ ACKNOWLEDGMENTS

These materials are based on work financed by the Croatian Foundation for Science (HRZZ grants 02.05/25 and IP-2014-09-6312), Croatian Ministry of Science Education and Sports (MZOS), the Natural Sciences and Engineering Research Council (NSERC) of Canada, and the University of Victoria.

■ REFERENCES

(1) *Carbonium Ions*; Olah, A. G., Schleyer, P. v. R., Eds.; Interscience Publishers: New York, 1968.

(2) Vogel, P. *Carbocation Chemistry*; Elsevier: Amsterdam, 1985.

(3) McClelland, R. A. In *Reactive Intermediate Chemistry*; Moss, R. A., Platz, M. S., Jones, M., Jr., Eds.; John Wiley & Sons: Hoboken, 2004.

(4) Olah, A. G. *J. Org. Chem.* **2001**, *66*, 5943–5957.

(5) Brown, H. C. *Acc. Chem. Res.* **1983**, *16*, 432–440.

(6) Olah, A. G.; Surya Prakash, G. K.; Saunders, M. *Acc. Chem. Res.* **1983**, *16*, 440–448.

(7) Walling, C. *Acc. Chem. Res.* **1983**, *16*, 448–454.

(8) Das, P. K. *Chem. Rev.* **1993**, *93*, 119–144.

(9) McClelland, R. A. *Tetrahedron* **1996**, *52*, 6823–6858.

(10) Kropp, P. J. *Acc. Chem. Res.* **1984**, *17*, 131–137.

(11) Freccero, M.; Fagnoni, M.; Albini, A. *J. Am. Chem. Soc.* **2003**, *125*, 13182–13190.

(12) Lazzaroni, S.; Dondi, D.; Fagnoni, M.; Albini, A. *J. Org. Chem.* **2008**, *73*, 206–211.

(13) Lazzaroni, S.; Dondi, D.; Fagnoni, M.; Albini, A. *J. Org. Chem.* **2010**, *75*, 315–323.

(14) Fagnoni, M.; Albini, A. *Acc. Chem. Res.* **2005**, *38*, 713–721.

(15) Dichiarante, V.; Fagnoni, M.; Albini, A. *Green Chem.* **2009**, *11*, 942–945.

(16) Dichiarante, V.; Fagnoni, M. *Synlett* **2008**, *2008*, 787–800.

DOI: 10.1021/acs.joc.5b02297
J. Org. Chem. 2015, 80, 12420–12430

(17) Rajesh, C. S.; Givens, R. S.; Wirz, J. *J. Am. Chem. Soc.* **2000**, *122*, 611−618.
(18) Zimmerman, H. E.; Sandel, V. R. *J. Am. Chem. Soc.* **1963**, *85*, 915−922.
(19) Zimmerman, H. E. *J. Am. Chem. Soc.* **1995**, *117*, 8988−8991.
(20) Diao, L.; Yang, C.; Wan, P. *J. Am. Chem. Soc.* **1995**, *117*, 5369−5370.
(21) Wan, P.; Barker, B.; Diao, L.; Fisher, M.; Shi, Y.; Yang, C. *Can. J. Chem.* **1996**, *74*, 465−475.
(22) Basarić, N.; Mlinarić-Majerski, K.; Kralj, M. *Curr. Org. Chem.* **2014**, *18*, 3−18.
(23) Ireland, J. F.; Wyatt, P. A. H. *Adv. Phys. Org. Chem.* **1976**, *12*, 131−221.
(24) Arnaut, L. G.; Formosinho, S. J. *J. Photochem. Photobiol., A* **1993**, *75*, 1−20.
(25) Klöpffer, W. *Adv. Photochem.* **1977**, *10*, 311−358.
(26) Formosinho, S. J.; Arnaut, L. G. *J. Photochem. Photobiol., A* **1993**, *75*, 21−48.
(27) Ormson, S. M.; Brown, R. G. *Prog. React. Kinet.* **1994**, *19*, 45−91.
(28) Le Gourrierec, D.; Ormson, S. M.; Brown, R. G. *Prog. React. Kinet.* **1994**, *19*, 211−275.
(29) Kasha, M. *J. Chem. Soc., Faraday Trans. 2* **1986**, *82*, 2379−2392.
(30) Basarić, N.; Žabčić, I.; Mlinarić-Majerski, K.; Wan, P. *J. Org. Chem.* **2010**, *75*, 102−116.
(31) Lenoir, D.; Hall, R. E.; Schleyer, P.v.R. *J. Am. Chem. Soc.* **1974**, *96*, 2138−2148.
(32) Lenoir, D.; Raber, D. J.; Schleyer, P.v.R. *J. Am. Chem. Soc.* **1974**, *96*, 2149−2156.
(33) Lenoir, D.; Mison, P.; Hyson, E.; von Schleyer, P. R.; Saunders, M.; Vogel, P.; Telkowski, L. A. *J. Am. Chem. Soc.* **1974**, *96*, 2157−2164.
(34) Schleyer, P. v. R.; Lenoir, D.; Mison, P.; Liang, G.; Surya Prakash, G. K.; Olah, G. A. *J. Am. Chem. Soc.* **1980**, *102*, 683−691.
(35) Herpers, E.; Krimse, W. *J. Chem. Soc., Chem. Commun.* **1993**, 160−161.
(36) Adams, D. A.; Bailey, P. D.; Collier, I. D.; Leah, S. A. H.; Ridyard, C. *Chem. Commun.* **1996**, 333−334.
(37) Majerski, Z.; Hameršak, Z. *Org. Synth.* **1979**, *59*, 147−150.
(38) Schleyer, P.v.R.; Funke, E.; Liggero, S. H. *J. Am. Chem. Soc.* **1969**, *91*, 3965−3967.
(39) Mirrington, R. N.; Feutrill, G. I. *Org. Synth.* **1973**, *53*, 90−93.
(40) Brousmiche, D. W.; Xu, M.; Lukeman, M.; Wan, P. *J. Am. Chem. Soc.* **2003**, *125*, 12961−12970.
(41) Diao, L.; Wan, P. *Can. J. Chem.* **2008**, *86*, 105−118.
(42) Basarić, N.; Cindro, N.; Bobinac, D.; Uzelac, L.; Mlinarić-Majerski, K.; Kralj, M.; Wan, P. *Photochem. Photobiol. Sci.* **2012**, *11*, 381−396.
(43) Pines, E. In *The Chemistry of Phenols*; Rappoport, Z., Ed.; Wiley: New York, 2003.
(44) Montalti, M.; Credi, A.; Prodi, L.; Gandolfi, M. T. *Handbook of Photochemistry*; CRC Taylor and Francis: Boca Raton, FL, 2006.
(45) Land, E. J.; Porter, G.; Strachan, E. *Trans. Faraday Soc.* **1961**, *57*, 1885−1893.
(46) Levin, P. R.; Khudyakov, I. V.; Kuz'min, V. A.; Hageman, H. J.; de Jonge, C. R. H. I. *J. Chem. Soc., Perkin Trans. 2* **1981**, 1237−1239.
(47) Shukla, D.; Schepp, N. P.; Mathivanan, N.; Johnston, L. J. *Can. J. Chem.* **1997**, *75*, 1820−1829.
(48) McClelland, R. A.; Chan, C.; Cozens, F. L.; Modro, A.; Steenken, S. *Angew. Chem., Int. Ed. Engl.* **1991**, *30*, 1337−1339.
(49) Cozens, F. L.; Kanagasabapathy, V. M.; McClelland, R. A.; Steenken, S. *Can. J. Chem.* **1999**, *77*, 2069−2082.
(50) Glasovac, Z.; Antol, I.; Vazdar, M.; Margetić, D. *Theor. Chem. Acc.* **2009**, *124*, 421−430.
(51) Michl, J. *J. Am. Chem. Soc.* **1996**, *118*, 3568−3579.
(52) Perrotta, R. R.; Winter, A. H.; Falvey, D. E. *Org. Lett.* **2011**, *13*, 212−215.
(53) Buck, A. T.; Beck, C. L.; Winter, A. H. *J. Am. Chem. Soc.* **2014**, *136*, 8933−8940.
(54) Smith, M. B.; March, J. *March's Advanced Organic Chemistry*; John Wiley: Hooboken, 2007.
(55) Liao, Y.; Bohne, C. *J. Phys. Chem.* **1996**, *100*, 734−743.
(56) Frisch, M. J.; Trucks, G. W.; Schlegel, H. B.; Scuseria, G. E.; Robb, M. A.; Cheeseman, J. R.; Montgomery, J. A., Jr.; Vreven, T.; Kudin, K. N.; Burant, J. C.; Millam, J. M.; Iyengar, S. S.; Tomasi, J.; Barone, V.; Mennucci, B.; Cossi, M.; Scalmani, G.; Rega, N.; Petersson, G. A.; Nakatsuji, H.; Hada, M.; Ehara, M.; Toyota, K.; Fukuda, R.; Hasegawa, J.; Ishida, M.; Nakajima, T.; Honda, Y.; Kitao, O.; Nakai, H.; Klene, M.; Li, X.; Knox, J. E.; Hratchian, H. P.; Cross, J. B.; Adamo, C.; Jaramillo, J.; Gomperts, R.; Stratmann, R. E.; Yazyev, O.; Austin, A. J.; Cammi, R.; Pomelli, C.; Ochterski, J. W.; Ayala, P. Y.; Morokuma, K.; Voth, G. A.; Salvador, P.; Dannenberg, J. J.; Zakrzewski, V. G.; Dapprich, S.; Daniels, A. D.; Strain, M. C.; Farkas, O.; Malick, D. K.; Rabuck, A. D.; Raghavachari, K.; Foresman, J. B.; Ortiz, J. V.; Cui, Q.; Baboul, A. G.; Clifford, S.; Cioslowski, J.; Stefanov, B. B.; Liu, G.; Liashenko, A.; Piskorz, P.; Komaromi, I.; Martin, R. L.; Fox, D. J.; Keith, T.; Al-Laham, M. A.; Peng, C. Y.; Nanayakkara, A.; Challacombe, M.; Gill, P. M. W.; Johnson, B.; Chen, W.; Wong, M. W.; Gonzalez, C.; Pople, J. A. *Gaussian 03*, revision E.01; Gaussian, Inc.: Pittsburgh, PA, 2003.
(57) Zhao, Y.; Truhlar, D. G. *Theor. Chem. Acc.* **2008**, *120*, 215−241.
(58) Frisch, M. J.; et al. *Gaussian 09*, revision D.01; Gaussian, Inc.: Wallingford, CT, 2013.
(59) Marenich, A. V.; Cramer, C. J.; Truhlar, D. G. *J. Phys. Chem. B* **2009**, *113*, 6378−6396.
(60) Pedretti, A.; Villa, L.; Vistoli, G. *J. Comput.-Aided Mol. Des.* **2004**, *18*, 167−173.
(61) Schaftenaar, G.; Noordik, J. H. *J. Comput.-Aided Mol. Des.* **2000**, *14*, 123−134.
(62) Oxford Diffraction Ltd. *Xcalibur CCD System, CrysAlis Software System, Versions 1.171.32*; Abingdon: Oxfordshire, England, 2008.
(63) Sheldrick, G. M. *Acta Crystallogr., Sect. A: Found. Crystallogr.* **2008**, *A64*, 112−122.
(64) Farrugia, L. J. *J. Appl. Crystallogr.* **1999**, *32*, 837−838.
(65) Farrugia, L. J. *J. Appl. Crystallogr.* **1997**, *30*, 565.

DOI: 10.1021/acs.joc.5b02297
J. Org. Chem. 2015, 80, 12420−12430